Tautomerization of Nucleobase Model Compounds: The 4-Pyridinol and 4(1*H*)-Pyridinone Monomers and Their Dimers

Jeffrey R. Reimers,*,† Lachlan E. Hall,†,‡ and Noel S. Hush†,§

School of Chemistry and Department of Biochemistry, University of Sydney, NSW 2006, Australia

Received: November 10, 1999; In Final Form: February 28, 2000

Nucleobases are important in many biochemical pathways, and one of their key features is that low-energy tautomerization processes can cause large changes in their chemical properties. Similar effects are also seen for photovoltaic molecules such as quinacridones, except that, in these systems, tautomerization is achieved through intermolecular proton transfer. An excellent model for both of these systems is the tautomerization between the 4-pyridinol and 4(1*H*)-pyridinone monomers and their dimers. Indeed, 4-pyridinol is known to be the most stable monomer in the gas phase, while chemically diverse 4(1*H*)-pyridinone is the most stable monomer both neat and in solution in polar solvents. We evaluate the energetics of gas-phase tautomerization of both monomers and dimers of these molecules using B3LYP, HCTH, SCF, MP2, MP4, QCISD, CCSD, and CCSD(T) methodologies. For the monomers, estimates of the CCSD(T)/aug-cc-pVTZ energies are obtained, while for the dimers, estimates of basis-set-superposition-error-corrected CCSD/aug-cc-pVDZ energies are obtained. Vibrational analyses are performed at the B3LYP/cc-pVDZ level to determine zero-point energy corrections and OH- and NH-stretch vibrational frequency changes. The hydrogen-bond energies show a clear preference for 4(1*H*)-pyridinone-containing dimers, and the dimer in which 4-pyridinol donates a hydrogen bond to 4(1*H*)-pyridinone is calculated to be only slightly higher in energy than the 4-pyridinol dimer.

1. Introduction

Tautomerization is a very important property in biological systems that is particularly relevant for nucleobases,[1−4] and many studies have been performed to investigate the tautomerization and association properties of the simplest model compounds,[5] the hydroxy pyridines. These compounds are also model systems for the study of the properties of larger molecules such as quinolones,[6] anthraquinones,[7] pyridonophanes,[8] and quinacridones,[9,10] many of which are of interest for their optical and photovoltaic[7,11,12] properties. Our concern here is with 4-pyridinol and 4(1*H*)-pyridinone,

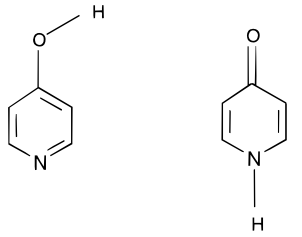

4-pyridinol 4(1*H*)-pyridinone

which are hydroxy (HYD) and oxo (OXO) tautomers, respectively. The HYD form is, in fact, a lactim and is fully aromatic, whereas the OXO form is a lactam and is thus not expected to be aromatic. Chemically, however, the OXO form exhibits more aromatic than lactam character, but spectroscopically, the OXO form exhibits typical lactam (or quinone) properties[13] and absorbs at a much lower energy than does the HYD form.[14] In quinacridones, tautomerization moves the main absorption band between the UV and visible regions, and hence, these molecules can function as a chemically controllable color switch.[15] Furthermore, these molecules self-associate in head-to-tail chains,[9] and hence, it is possible to envisage[15] their use in the construction of a micro electrochemical solid-state color display device. For such systems, 4(1*H*)-pyridinone is an excellent model compound, not only because of its analogous tautomeric and optical properties but also because of its associative properties, with its prevalent OXO tautomer being known to associate into chains of up to >30 monomer units in aqueous solution.[16,17] To direct the synthesis and hence explore the synthetic flexibility of quinacridones[10] and the like, it is important to understand the energetics of tautomerization of 4(1*H*)-pyridinone and its oligomers. Here, we investigate monomers and dimers of this compound through extensive ab initio and density-functional computation.

An important aspect of the tautomerization of 4(1*H*)-pyridinone is its sensitivity to environment. In the gas phase, this molecule is known to exist to within experimental detection limits purely in its HYD form.[14,18] However, in aqueous solution, it exists in its OXO form. This is easily understood in terms of solvation effects, using either cluster[19−22] or reaction-field[23] methodologies, with the HYD form becoming the most important form in solvents of low polarity.[17,23,24] Related systems such as quinolones are interesting in that it is possible to obtain widely varying nonequilibrium gas-phase compositions by varying the mode of production of the vapor.[25] These effects are not of concern to us here, however, and we concentrate on the determination of the gas-phase equilibrium properties of 4(1*H*)-pyridinone and its dimers.

* To whom correspondence should be addressed. E-mail: reimers@chem.usyd.edu.au.

† School of Chemistry.

‡ Current address: Molecular Electronics Research, 393 Darling St., Balmain 2041, Australia.

§ Department of Biochemistry.

10.1021/jp9939827 CCC: $19.00
Published on Web 04/27/2000

TABLE 1: Energy ΔE of 4(1*H*)-Pyridinone with Respect to 4-Pyridinol and Barrier $\Delta E^{\ddagger}$ for Free Rotation of the Hydroxyl Proton in 4-Pyridinol[a]

property[b]	basis set	SCF	SCF[c]	MP2[d]	MP2	MP2[c]	MP4[c]	QCISD[c]	CCSD[c]	CCSD(T)[c]	HCTH[c]	B3LYP
ΔE	3-21G	0.7			−1.5							−3.6
	cc-pVDZ	4.1	4.3	5.3	5.5	5.5	2.6	3.2	3.9	4.1	0.6	2.1
	aug-cc-pVDZ		3.8			4.8			3.2	3.4		1.9[c]
	cc-pVTZ	2.7	3.6			5.4			3.6	3.9		1.7[c]
	aug-cc-pVTZ		3.1			4.7			[2.9]	[3.2]	0.6	1.5[c]
$\Delta E^{\ddagger}$	3-21G	3.5			4.4							5.4
	cc-pVDZ	4.3		4.9	4.8	4.9	4.8	4.9	4.7	4.8	6.1	5.5
	cc-pVTZ	4.3	4.3			4.6			4.5	4.7		5.1[c]

[a] Geometries are optimized using the indicated method unless noted otherwise. The reported[28] MP2/6-31++G** value at the SCF/6-31++G** geometry is 5.3 kcal mol^{-1}. [b] Values are in kilocalories per mole. [c] B3LYP/cc-pVDZ optimized geometry used. [d] SCF/3-21G optimized geometry used.

Both this system and other, closely related[5,22,26−30] monomeric systems have frequently been investigated by theoretical means. Early semiempirical[19] and ab initio SCF[31−33] calculations produced qualitatively reasonable descriptions of the tautomerization, but significant quantitative differences have been found at the correlated MP2 level.[28,34,35] The recent development of density-functional techniques has added another perspective, with most,[29,36,37] but not all,[26] indications suggesting that the B3LYP[38] functional should give realistic results for systems such as this. Also, new functions such as HCTH[39] have been parametrized with hydrogen-bonding interactions included in the training set. As we are concerned with the identification of the most computationally effective method for examining tautomerization in systems much larger than this, we perform calculations using B3LYP, HCTH, and SCF methodologies. In addition, we consider results from MP2,[40] MP4,[41] QCISD,[42] and extensive coupled cluster CCSD[43] and CCSD(T)[44] calculations.

2. Methods

A variety of basis sets were employed, ranging from the small 3-21G basis set through the correlation-consistent basis sets cc-pVDZ,[45] aug-cc-pVDZ,[46] cc-pVTZ,[45] and aug-cc-pVTZ.[46] All B3LYP calculations were performed using Gaussian-94,[47] as were all SCF and MP2 geometry optimizations and analytical frequency calculations. The single-point energy calculations at the SCF, MP2, MP4, QCISD, CCSD, and CCSD(T) levels were performed using MOLPRO-97,[48] and the HCTH calculations were performed using a beta-release version of CADPAC6.5.[49] The very large MP2 calculations (using the aug-cc-pVDZ basis set for dimers and the aug-cc-pVTZ basis set for monomers) were performed using TURBOMOLE[50] with the TZVPP auxiliary basis set.[51] Calculations to test the accuracy of the use of auxiliary basis sets[51] in these MP2 calculations were performed for high-symmetry species, as well as for the water dimer, and the errors in the relative energies found to be less that 0.03 kcal mol^{-1}.

3. Monomers

Calculated properties for the 4(1*H*)-pyridinone and 4-pyridinol monomers are shown in Tables 1 and 2, while all optimized coordinates are given in full in the Supporting Information. First, in Table 1 are shown the calculated energies, ΔE, of 4(1*H*)-pyridinone with respect to the planar optimized structure of 4-pyridinol, as well as the barriers, $\Delta E^{\ddagger}$, to free rotation of the hydroxyl proton. All methods produce similar values for the hydroxy rotation barrier, and it appears that this barrier is reasonably small, ca. 4.7 kcal mol^{-1}, indicating that strong hydrogen bonding of the hydroxyl proton could induce significant deviations from planarity. The calculated relative energies of the tautomers vary significantly, however, with these results being consistent with results from earlier SCF and MP2 calculations.[28,31−35] Clearly, the small 3-21G basis set should not be used for accurate energy calculations, though the MP2-calculated energies at the SCF/3-21G optimized geometries closely parallel those at the MP2 optimized geometries; hence, this basis set may be useful in geometric calculations on larger oligomers.[15] Using the polarized double-ζ cc-pVDZ basis set, ΔE increases from 4.1 to 5.5 kcal mol^{-1} in going from SCF to MP2, but higher treatments of correlation appear to be poorly convergent, with results of 2.6 (MP4), 3.2 (QCISD), 3.9 (CCSD), and 4.1 kcal mol^{-1} [CCSD(T)]. The effects of systematic enlargement of the basis set, through expansion to triple-ζ and/or addition of augmented functions, appear well-behaved, however, with the two effects being additive at the SCF, MP2, and B3LYP levels and with the total corrections being −1.2, −0.8, and −0.6 kcal mol^{-1}, respectively. At the CCSD and CCSD(T) levels, use of the doubly expanded basis set (aug-cc-pVTZ) was not currently feasible, but the sums of the individual corrections are −1.0 and −0.9 kcal mol^{-1}, respectively, results that are quite similar to those for MP2. Hence, we estimate the CCSD(T)/aug-cc-pVTZ value of ΔE to be 3.2 kcal mol^{-1}, a result that we take as our best estimate of the actual molecular property.

TABLE 2: Calculated Dipole Moments μ and Polarizability Components α for the 4-Pyridinol (HYD) and 4-Pyridinone (OXO) Tautomers[a]

property[b]	SCF	SCF[c]	MP2	MP2[c]	CCSD[c]	CCSD(T)[c]	B3LYP
$\lvert\mu^{HYD}\rvert$	2.6	2.57	2.71	2.72	2.62	2.62	2.71
μ^{OXO}	6.91	7.24	6.43	6.34	6.41	6.33	6.54
α_{LL}^{HYD}		70		70.7	71.6	72.4	74.8
α_{LS}^{HYD}		−1.5		−2.5	−1.6	−1.6	−1.9
α_{SS}^{HYD}		69.6		72.5	70.4	70.9	73.7
α_{NN}^{HYD}		25.2		24.9	24.9	24.9	25.2
α_{LL}^{OXO}		84.6		90.9	84.9	85.3	84.3
α_{SS}^{OXO}		58.9		71.2	61.9	63.6	66.4
α_{NN}^{OXO}		25.2		31.4	24.6	25	25.3

[a] All calculations are performed using the cc-pVDZ basis set at geometries optimized using the indicated method unless noted otherwise. Inertial coordinates are used with *L* being the long axis (the O−N direction for 4-pyridinone and approximately the same for 4-pyridinol), *S* the short axis, and *N* the axis normal to the molecular plane. [b] μ in Debye and α in au. [c] B3LYP/cc-pVDZ optimized geometry used.

Thermal and zero-point vibrational corrections to the tautomerization energy ΔE have been evaluated at both the MP2 and the B3LYP levels using the cc-pVDZ basis set through normal-mode analysis. All calculated normal modes and vibrational frequencies are given in full in the Supporting Information. The calculated zero-point energy corrections of 0.15 (MP2) and 0.26 kcal mol^{-1} (B3LYP) are both much smaller than the SCF value[34] of 0.7 kcal mol^{-1}. We thus take the best-estimate zero-

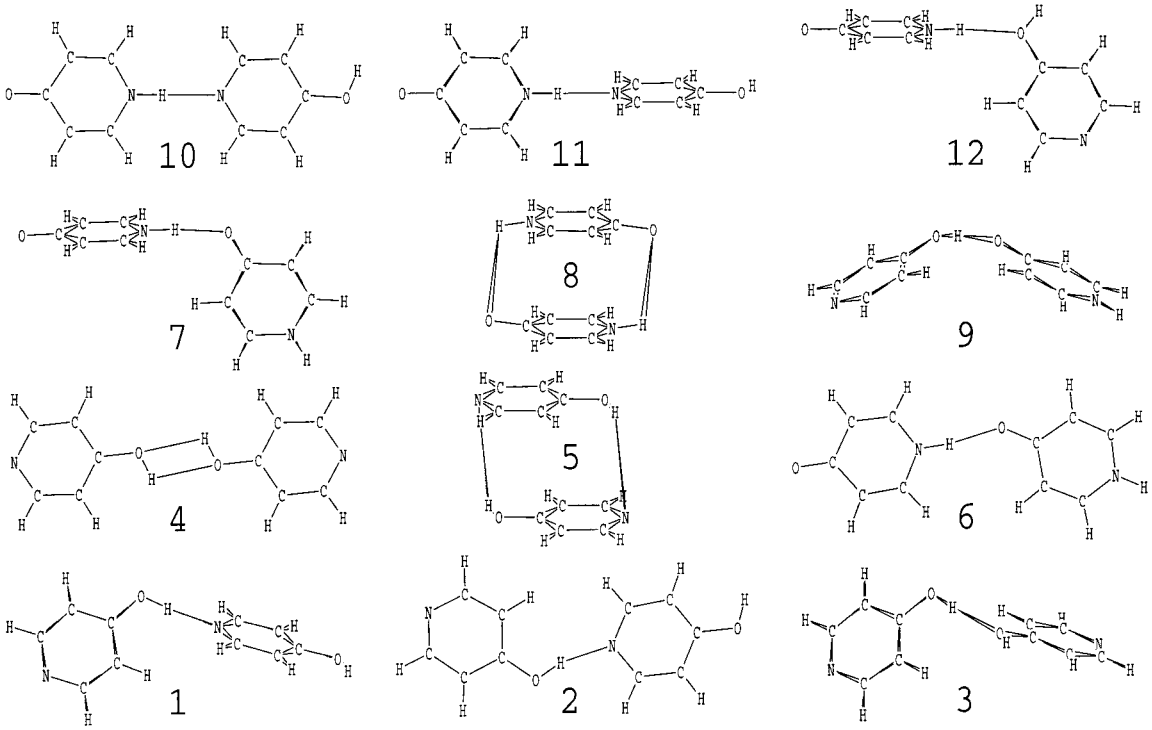

Figure 1. B3LYP/cc-pVDZ optimized structures of the 12 dimers described in Tables 3 and 4.

point energy corrected value of ΔE to be 3.4 kcal mol^{-1}. Experimentally, 4-pyridinol is known[18] to have the lowest energy in the gas phase, with the free-energy difference at 298 K, ΔG^{298}, exceeding 2 kcal mol^{-1}. The calculated entropy changes are -0.83 (MP2) and -0.86 cal mol^{-1} K^{-1} (B3LYP), while the calculated total changes to the Gibbs free energy at 298 K are 0.45 (MP2) and 0.57 kcal mol^{-1} (B3LYP). Hence, our best estimate for ΔG^{298} is 3.7 kcal mol^{-1}, a value which, in fact, does exceed its experimental lower bound. Of all the computational methods employed, only HCTH produced energy differences that are clearly inconsistent with the available experimental data. The apparent underestimation of ΔE by ca. 3 kcal mol^{-1} for HCTH is, however, within the expected accuracy[39] of this multipurpose functional.

In Table 2 are shown calculated values for the dipole moment and polarizability of 4-pyridinol and 4(1*H*)-pyridinone evaluated using the cc-pVDZ basis set. For the SCF and B3LYP methods, analytical expressions for these quantities were used, whereas numerical differentiation with respect to an applied electric field was used for the MP2, CCSD, and CCSD(T) methods. To test the accuracy of this numerical procedure, this method was also applied for B3LYP, and errors of less than 1% were found. This result is much less than the variation of ca. 15% that was found in the calculated properties as the treatment of electron correlation is varied, indicating that the method is sufficiently accurate for our purposes. In general, the B3LYP results closely parallel those from CCSD. Variations of the calculated properties as a function of basis set are not included in the table, however, and in particular, the addition of augmented basis sets is expected to have significant quantitative effects. To test this hypothesis, B3LYP calculations of the dipole moment were repeated using the aug-cc-pVDZ and aug-cc-pVTZ basis sets: the calculated dipole moments of 4-pyridinol and 4(1*H*)-pyridinone changed from 2.71 and 6.54 D (cc-pVDZ) to 2.70 and 6.96 D (aug-cc-pVDZ) to 2.70 and 6.95 D (aug-cc-pVTZ), respectively. Larger effects are expected for the calculated polarizabilities, however. Nevertheless, the dipole moment of 4-pyridinol is calculated to be very much smaller than that of 4(1*H*)-pyridinone, while the corresponding polarizabilities are only slightly smaller. These results support the conclusion, which has been perhaps most evident from recent reaction-field studies,[23] that dipole−dipole solvation effects are responsible for the lower free energy of 4(1*H*)-pyridinone dissolved in polar solvents.

4. Dimers

The geometries for 12 dimers of 4-pyridinol and/or 4(1*H*)-pyridinone were optimized at the SCF/3-21G, B3LYP/cc-pVDZ, and MP2/cc-pVDZ levels. Included in these structures are those of HYD → HYD, HYD → OXO, OXO → HYD, and OXY → OXO hydrogen-bond donation patterns. All resultant structures are given in full in the Supporting Information, while the B3LYP/cc-pVDZ structures are shown in Figure 1. Basically, the corresponding structures obtained using the three methods are all qualitatively similar. There is a notable exception, however, in the SCF energies for the stacked structures **5** and **8**. For these dimers, the inter-ring distances are much shorter in the MP2/cc-pVDZ structures than in the SCF/3-21G and B3LYP/cc-pVDZ structures. Naively, one would expect that the MP2 results would be the most reliable, as only this method properly includes important dispersion interactions. However, as discussed later, CCSD/cc-pVDZ calculations suggest that MP2 considerably overestimates the magnitude of the interactions, and hence, we select the set of 12 B3LYP/cc-pVDZ structures for subsequent analysis.

Single-point energy calculations have been performed using augmented basis sets, MP2/aug-cc-pVDZ and B3LYP/aug-cc-pVDZ. Counterpoise-corrected hydrogen-bond energies E_{HB} are shown in Table 3, along with the appropriate root-mean-square (RMS) basis-set superposition errors (BSSE). The effects of adding the augmented functions to the B3LYP calculation are small, the most significant being a reduction of the RMS BSSE to just 0.7 kcal mol^{-1}. This result is typical of density-functional

TABLE 3: Calculated Hydrogen-Bond Strengths E_{HB} for Various Dimers of 4-Pyridinol and/or 4(1H)-Pyridinone and Root-Mean-Square Basis-Set-Superposition Error (BSSE)[a]

			E_{HB}, kcal mol^{-1}												
molecule		structured	SCF 3-21G[b]	SCF avdz[c]	SCF vdz[b]	SCF vdz[d]	SCF vdz[c]	MP2 avdz[c]	MP2 vdz[b]	MP2 vdz[d]	MP2 vdz[c]	CCSD vdz[c]	HCTH vdz[c]	B3LYP vdz[c]	B3LYP avdz[c]
$NC_5H_4OH\cdots NC_5H_4OH$	**1**	twisted, C_1	−10.7	−6.7	−6.7	−6.4	−6.7	−11.2	−9.7	−9.7	−9.7		−6.6	−9.5	−9.6
	2	planar, C_s	−10.5	−3.7	−6.5	−6.3	−6.3	−11.1	−9.4	−9.5	−9.4	−8.8	−6.4	−9.2	−9.1
$NC_5H_4OH\cdots OHC_5H_4N$	**3**	single HB,[e] C_1	−5.6	−2.3	−0.7	−1.3	−2.6	−5.5	−3.4	−4.4	−4.5		0.0	−3.5	−3.4
	4	double HB,[e] C_2	−3.8	−2	−1.5	−2.4	−2.4	−3.6	−2.3	−3.1	−3.0		0.1	−2.5	−2.5
NC_5H_4OH ⋮ HOC_5H_4N	**5**	stacked, C_i	−0.1	−0.1	0	7.8	0.1	−6.3	−4.1	−3.9	−4.3	−2.6	1.7	−0.5	−0.4
$HNC_5H_4O\cdots HNC_5H_4O$	**6**	planar, C_s	−10.7	−8.8	−8.6	−8.2	−8.6	−12	−10.5	−10.2	−10.4		−7.6	−10.2	−10.6
	7	perp., C_s	−11	−8.8	−8.4	−7.6	−8.4	−12.9	−11	−10.6	−10.8	−9.8	−7.7	−10.5	−10.9
HNC_5H_4O ⋮ OC_5H_4NH	**8**	stacked, C_{2h}	−2.1	−3	−2.7	2.7	−2.6	−10.4	−7.1	−6.6	−7.2	−2.6	−0.1	−2.7	−3.5
$NC_5H_4OH\cdots OC_5H_4NH$	**9**	twisted, C_1	−11.5	−8.6	−7.6	−7.1	−8.5	−13.6	−10.8	−10.9	−11.1	−9.5	−7.3	−11.3	−11.7
$OC_5H_4NH\cdots NC_5H_4OH$	**10**	planar, C_s	−8.4	−11.9	−5.9	−5.5	−5.7	−9.7	−9.0	−8.9	−9		−6.0	−8	−7.8
	11	perp., C_s	−9.4	−12.8	−6.6	−5.8	−6.4	−10.5	−9.5	−9.2	−9.5	−8.5	−6.6	−8.7	−8.8
$OC_5H_4NH\cdots OHC_5H_4N$	**12**	twisted, C_1	−5.4	−2.3	−1.9	−2	−2.6	−5.1	−4.2	−4.3	−4.4		−0.9	−3.3	−3.1
RMS BSSE	−	−	4.4	0.6	2	2.3	1.9	2.4	3.8	4.4	3.6	3.9	2.5	2.8	0.7

[a] B3LYP/cc-pVDZ optimized geometries are shown in Figure 1. The basis sets used are vdz, cc-pVDZ; vtz, cc-pVTZ; avdz, aug-cc-pVDZ; and avtz, aug-cc-pVTZ. [b] SCF/3-21G optimized geometry used. [c] B3LYP/cc-pVDZ optimized geometry used. [d] MP2/vdz optimized geometry used. [e] HB = hydrogen bond.

calculations of hydrogen-bond energies and, indeed, parallels the results already obtained for the monomers themselves. Much larger basis-set dependences are found at the MP2 level, however, and by analogy with the monomer results, we expect that the effects of enlarging the basis set on CCSD and CCSD(T) calculations would parallel these larger dependences.

Hydrogen-bond energies obtained using the CCSD/cc-pVDZ and HCTH/cc-pVDZ methods are also shown in Table 3; these energies are evaluated as the difference between the dimer energy and the sum of the monomer energies at the optimized B3LYP/cc-pVDZ geometries. Overall, the results from all of the methods show the same basic trends, with the MP2 and B3LYP hydrogen-bond energies being typically 1−2 kcal mol^{-1} more attractive than the CCSD energies, which are, themselves, ca. 2 kcal mol^{-1} more attractive than the HCTH energies. Significant differences do appear for structures **5** and **8**. For **8**, the HCTH, B3LYP, and CCSD results differ from the MP2 results by 4.6−7.1 kcal mol^{-1}, and the B3LYP and HCTH results appear to track those from CCSD better than do the MP2 results.

Although the efficient SCF/3-21G method appears to produce reliable geometries, a feature that we have exploited elsewhere[15] in calculations of the structure of trimers, tetramers, and hexamers, its hydrogen-bond energies are poorly converged with respect to expansion of the basis set to cc-pVDZ and aug-cc-pVDZ. Interestingly, through cancellation of errors, it appears that it is the SCF/3-21G energies that are in best agreement with the MP2, B3LYP, and CCSD calculations.

The largest hydrogen-bond strengths predicted using CCSD and HCTH are for the pyridinone−pyridinone dimers **6** and **7**, with that for the dimer **9**, in which a pyridinol donates a hydrogen bond to a pyridinone, just 0.3 kcal mol^{-1} less attractive. For MP2 and B3LYP, the results are similar, except that the order is reversed. The interactions between two pyridinols (structures **1** and **2**) and the dimers in which a pyridinone donates a hydrogen bond to a pyridinol (structures **10** and **11**) are predicted to be ca. 1 kcal mol^{-1} weaker. It is interesting to note that, for **9**, the MP2 and CCSD BSSE is ca. 6 kcal mol^{-1}, 50% larger than for any other structure, and that the largest MP2 change of −2.5 kcal mol^{-1} is found for this structure on enlarging the basis set to aug-cc-pVDZ. For all methods, structures **3**, **4**, and **12**, in which a hydroxy group acts as a hydrogen-bond acceptor, have hydrogen-bond energies that are ca. 7 kcal mol^{-1} less attractive than those for the other hydrogen-bond types, and thus, these structures are not likely to be important. Similarly, the stacked structures **5** and **8** are also high in energy, but sufficient binding is predicted at the CCSD level to suggest that these interactions may have an important role in determining the geometry of condensed phases.

Normal-coordinate analysis on all 12 structures has been performed using B3LYP/cc-pVDZ, and again, all results are given in full in the Supporting Information. Zero-point (ZPT) energies, additional corrections to the enthalpy (ΔH_{corr}^{298}), and entropies (ΔS) are listed in Table 4, however, along with corrected CCSD, MP2, HCTH, and B3LYP estimates for the relative absolute energies of the 12 structures, ΔE_2. These estimates are obtained by taking from Table 1 the best estimate of 3.2 kcal mol^{-1} for the monomer energy difference ΔE, adding this to the CCSD/cc-pVDZ, MP2/cc-pVDZ, HCTH/cc-pVDZ, and B3LYP/cc-pVDZ hydrogen-bond energies from Table 3, adding a correction to account for basis-set expansion (obtained as the difference between the MP2/aug-cc-pVDZ and MP2/cc-pVDZ results from Table 3), and adding the B3LYP/cc-pVDZ ZPT correction from Table 4. Once again, all four sets of results are similar, and with the exception of the stacked structures **5** and **8** for which MP2 appears to overestimate the binding, the estimated relative energies agree to within 1 kcal mol^{-1}. The thermodynamic properties ΔH_{corr}^{298} and ΔS provide an indication of the variability of the relative stability of the complexes as the temperature increases. Note, however, that these quantities were obtained using a harmonic vibrational analysis, and as the dimers possess many hindered or free rotors, these results are only crude estimates.

The calculations show that, although 4-pyridinone is clearly the most stable monomeric structure, the increased hydrogen-bonding strength of the pyridinol−pyridinone complex makes this dimer only slightly higher in energy than the pure pyridinol dimer. Hence, even at the dimer level, intermolecular interactions are seen to favor the tautomerization of 4-pyridinol to 4(1*H*)-pyridinone. No other dimer structure is likely to be of sufficiently low energy to contribute significantly to a thermally equilibrated dimer sample.

TABLE 4: Characterization and Thermodynamic and Spectroscopic Properties of Various Dimers of 4-Pyridinol and/or 4(1H)-Pyridinone

						ΔE_2[a]					
molecule		structure	type	$\Delta\nu$,[c] cm^{-1}	ZPT corr[b]	CCSD	MP2	HCTH	B3LYP	ΔH_{corr}^{298} [b]	ΔS[b]
$NC_5H_4OH\cdots NC_5H_4OH$	**1**	twisted, C_1	min.	−566 (HB), −3.5 (F)	1.1		0.1	0.2	0.1	0.5	−36
	2	planar, C_s	TS	−548 (HB), −3.2 (F)	0.9	[0]	[0]	[0]	[0]	0.5	−36
$NC_5H_4OH\cdots OHC_5H_4N$	**3**	single HB, C_1	min.	−137 (HB), 3.1 (F)	1.0		5.7	6.1	5.3	1.2	−30
	4	double HB, C_2	TS	−27.3 (a), −25.1 (b)	0.5		7.1	6.3	6.6	0.3	−37
NC_5H_4OH ⋮ HOC_5H_4N	**5**	stacked, C_i	TS	−9.1 (g), −8.4 (u)	0.4	5.2	4.4	7.2	7.7	0.9	−33
$HNC_5H_4O\cdots HNC_5H_4O$	**6**	planar, C_s	TS	−319 (HB), −11.5 (F)	0.9		5.5	5.4	5.6	1.2	−24
	7	perp., C_s	min.	−409 (HB), −12.5 (F)	1.0	5.3	4.7	5.0	5.0	1.1	−27
HNC_5H_4O ⋮ OC_5H_4NH	**8**	stacked, C_{2h}	TS	−17.4 (a_g), −16.9 (b_u)	0.5	10.6	6.7	10.7	10.9	0.3	−38
$NC_5H_4OH\cdots OC_5H_4NH$	**9**	twisted, C_1	min.	−609 (HB), −12.7 (F)	1.4	1.9	1.2	1.7	0.5	0.9	−32
$OC_5H_4NH\cdots NC_5H_4OH$	**10**	planar, C_s	TS	−370 (HB), −8.2 (F)	0.8		4.5	4.5	5.3	0.6	−34
	11	perp., C_s	min.	−403 (HB), −3.2 (F)	0.9	4.2	3.8	3.7	4.4	1.2	−26
$OC_5H_4NH\cdots OHC_5H_4N$	**12**	twisted, C_1	min.	−101 (HB), −0.4 (F)	0.6		8.9	9.2	9.6	1.4	−23

[a] The zero-point energy change and the MP2-calculated correction for the basis-set expansion cc-pVDZ to aug-cc-pVDZ (from Table 3) are combined with the best-estimate monomer energy difference of 3.2 kcal mol^{-1} (from Table 1) and either the CCSD/cc-pVDZ or the 3LYP/cc-pVDZ hydrogen-bond energies E_{HB} (from Table 3) in order to estimate the relative energy of the dimers at 0 K, ΔE (in kcal mol^{-1}); see text. [b] The zero-point energy at finite temperature correction to the enthalpy, ΔH_{corr}^{298}, in kcal mol^{-1}, and the entropy change on dimerization, ΔS, in cal mol^{-1} K^{-1}, are evaluated within the harmonic vibrational approximation using B3LYP/cc-pVDZ; this vibrational analysis is also used to characterize each dimer as a local minimum (min.) or transition state (TS). [c] The change in vibration frequency $\Delta\nu$ on dimerization is evaluated as the difference between the B3LYP/cc-pVDZ calculated NH- and/or OH-stretch frequencies and the corresponding monomer values [3770 cm^{-1} for 4-pyridinol, 3648 cm^{-1} for 4(1*H*)-pyridinone]; the modes are either assigned as hydrogen-bond donor (HB) or free donor (F) bands or assigned by symmetry.

Also given in Table 4 are the calculated frequency changes of the NH- and OH-stretch vibrations due to dimer formation. Large frequency changes on the order of −600 cm^{-1} are associated with strong hydrogen bonding involving an OH group, while the corresponding change for a NH vibration is on the order of −350 cm^{-1}. Much smaller changes are predicted for the weakly bonded complexes, including those that involve hydrogen-bond donation to a hydroxy oxygen. The changes in the OH and NH vibrational bands are important markers, and these results may be useful in identifying experimentally produced dimers.

5. Conclusions

The a priori calculation of the properties of tautomeric systems is a difficult task, as the relative energies of the structures of interest are often very similar. It is clear that all of the computational methods considered herein predict the correct qualitative result that 4-pyridinol and 4(1*H*)-pyridinone are very close in energy. When the results obtained with the small 3-21G basis set are neglected, the SCF, MP2, MP4, QCISD, CCSD, CCSD(T), HCTH, and B3LYP methods predict 4(1*H*)-pyridinone to be 0.6−5.5 kcal mol^{-1} less stable that 4-pyridinone. This range is, however, an order of magnitude larger than the maximum permissible inaccuracy if calculations of this type are to be useful in the interpretation of experimental data. The previous calculated energy differences obtained using SCF and MP2 were significantly different, and our results obtained using density-functional theory, in fact, lie *outside* of their predicted range. Experimentally, the energy difference is known to exceed 2 kcal mol^{-1}, consistent with the SCF and MP2 results. However, at higher levels of theory such as CCSD and CCSD(T), the ab initio results appear to be converging toward a zero-point energy corrected value of 3.4 kcal mol^{-1}. This value is expected to provide a realistic estimate for this important but not yet properly unmeasured quantity.

Accurate computation of the properties of tautomeric dimers is an even more difficult task, as both the monomer energies and the intermolecular interaction energies must be calculated. We have simplified this process by performing the most accurate calculations possible for the isolated monomers, evaluating the interaction energy separately. After demonstrating that the fast auxiliary-basis-set RIMP2 method[51] is applicable to the evaluation of hydrogen-bond energies, we evaluated the interaction energies at the MP2 level using the large aug-cc-pVDZ basis set. Again, we found significant differences between MP2 and density-functional results, but in this case, CCSD calculations suggest that MP2 overestimates the intermolecular interactions, particularly for π-stacked configurations. Hence, the B3LYP and HCTH density-functional methods appear to be slightly more reliable.

Pyridinol−pyridinone tautomerization results in significant changes to the chemical reactivity, electrical conductivity, solvation, and spectroscopic properties of the molecules. The preferential solvation of the pyridinone form in polar solvents arises from the much larger dipole moment of this tautomer, as has been demonstrated previously in many ways. Here, we show that, even at the level of dimer formation, this effect applies. Furthermore our calculations predict that the 4-pyridinol dimer

and the mixed 4-pyridinol−4(1*H*)-pyridinone dimer have only a small energy difference (0.5, 1.2, 1.7, and 1.9 kcal mol^{-1} using B3LYP, MP2, CHTH, and CCSD, respectively). Hence, through the observation of the energetics of dimer formation, experimental tautomerization energies may be obtained more easily than they are for monomer tautomerization. Such experimental data would be very useful in calibrating computational techniques. We have presented key spectroscopic and thermodynamic properties that may aid in the experimental observation of such dimers, and in the Supporting Information provide a large range of additional information that may be useful for this and other purposes.

Acknowledgment. J.R.R. and L.E.H. thank the Australian Research Council for funding this work. We also thank Kia Silverbrook of Molecular Electronics Research, Balmain, Australia, for a discussion of possible applications.

Supporting Information Available: ASCII text describing all optimized structures and all deduced normal modes, vibration frequencies, infrared intensities, and other calculated results. This material is available free of charge via the Internet at http://pubs.acs.org.

References and Notes

(1) Cieplak, P.; Bash, P.; Singh, U. C.; Kollman, P. A. *J. Am. Chem. Soc.* **1987**, *109*, 6283.

(2) Katritzky, A. R.; Karelson, M. M.; Harris, P. A. *Heterocycles* **1991**, *32*, 329.

(3) Cramer, C. J.; Truhlar, D. G. *J. Am. Chem. Soc.* **1991**, *113*, 8552.

(4) Szafran, M.; Karelson, M. M.; Katritzky, A. R.; Roput, J.; Zerner, M. C. *J. Comput. Chem.* **1993**, *14*, 371.

(5) Smets, J.; Adamowicz, L.; Maes, G. *J. Mol. Struct. (THEOCHEM)* **1994**, *322*, 113.

(6) Bartolomei, M.; Cignitti, M.; Ramusino, M. C.; La Manna, G. *J. Mol. Struct. (THEOCHEM)* **1995**, *330*, 431.

(7) Quotschalla, U.; Hanemann, T.; Böhm, M. C.; Haase, W. *Mol. Cryst. Liq. Cryst. Sci. Technol.* **1991**, *207*, 103.

(8) Vögtle, F.; Breitenbach, J.; Nieger, M. *J. Chem. Soc., Chem. Commun.* **1991**, 860.

(9) Potts, G. D.; Jones, W.; Bullock, J. F.; Andrews, S. J. *J. Chem. Soc., Chem. Commun.* **1994**, 2565.

(10) Keller, U.; Müllen, K.; De Feyter, S.; De Schryver, F. C. *Adv. Mater. (Weinheim, Ger.)* **1996**, *8*, 490.

(11) Tomida, M.; Kusabayashi, S.; Yokoyama, M. *Chem. Lett.* **1987**, 609.

(12) Manabe, K.; Kusabayashi, S.; Yokoyama, M. *Chem. Lett.* **1984**, 1305.

(13) Reimers, J. R.; Hall, L. E.; Crossley, M. J.; Hush, N. S. *J. Phys. Chem. A* **1999**, *103*, 4385.

(14) Beak, P.; Fry, S. F., Jr.; Lee, J.; Steele, F. *J. Am. Chem. Soc.* **1976**, *98*, 171.

(15) Reimers, J. R.; Hall, L. E.; Hush, N. S.; Silverbrook, K. *Ann. N.Y. Acad. Sci.* **1998**, *852*, 38.

(16) Beak, P.; Covington, J. B.; Zeigler, J. M. *J. Org. Chem.* **1978**, *43*, 177.

(17) Beak, P.; Covington, J. B.; Smith, S. G.; White, J. M.; Zeigler, J. M. *J. Org. Chem.* **1980**, *45*, 1354.

(18) Cook, M. J.; El-Abbady, S.; Katritzky, A. R.; Guimon, C.; Pfister-Guillouzo, G. *J. Chem. Soc., Perkin Trans. 2* **1977**, 1652.

(19) Kwiatkowski, J. S.; Szczodrowska, B. *Chem. Phys.* **1978**, *27*, 389.

(20) Corongiu, G.; Clementi, E.; Dagnino, M.; Paoloni, L. *Chem. Phys.* **1979**, *40*, 439.

(21) Sordo, J. A.; Klobukowski, M.; Fraga, S. *J. Am. Chem. Soc.* **1985**, *107*, 7569.

(22) Li, G.-S.; Ruiz-López, M. F.; Maigret, B. *J. Phys. Chem.* **1997**, *101*, 7885.

(23) Wang, J.; Boyd, R. J. *Chem. Phys. Lett.* **1996**, *259*, 647.

(24) Frank, J.; Katritzky, A. R. *J. Chem. Soc., Perkin Trans. 2* **1976**, 1428.

(25) de la Cruz, A.; Elguero, J.; Goya, P.; Martinínez, A. *Tetrahedron* **1992**, *48*, 6135.

(26) Zhang, Q.; Bell, R.; Truong, T. N. *J. Phys. Chem.* **1995**, *99*, 592.

(27) Li, G.-S.; Ruiz-López, M. F.; Zhang, M.-S.; Maigret, B. *J. Mol. Struct. (THEOCHEM)* **1998**, *422*, 197.

(28) Buyl, F.; Smets, J.; Maes, G.; Adamowicz, L. *J. Phys. Chem.* **1995**, *99*, 14967.

(29) Liedl, K. R.; Sekušak, S.; Kroemer, R. T.; Rode, B. M. *J. Phys. Chem. A* **1997**, *101*, 4707.

(30) Sim, F.; St-Amant, A.; Papai, I.; Salahub, D. R. *J. Am. Chem. Soc.* **1992**, *114*, 4391.

(31) La Manna, G. *J. Mol. Struct. (THEOCHEM)* **1981**, *85*, 389.

(32) Scanlan, M. J.; Hillier, I. H.; Davies, R. H. *J. Chem. Soc., Chem. Commun.* **1982**, 685.

(33) Scanlan, M. J.; Hillier, I. H.; MacDowell, A. A. *J. Am. Chem. Soc.* **1983**, *105*, 3568.

(34) Schlegel, H. B.; Gund, P.; Fluder, E. M. *J. Am. Chem. Soc.* **1982**, *104*, 5347.

(35) Kwiatkowski, J. S.; Bartlett, R. J.; Person, W. B. *J. Am. Chem. Soc.* **1988**, *110*, 2353.

(36) Rablen, P. R.; Lockman, J. W.; Jorgensen, W. L. *J. Phys. Chem. A* **1998**, *102*, 3782.

(37) Reimers, J. R.; Hall, L. E. *J. Am. Chem. Soc.* **1999**, *121*, 3730.

(38) Becke, A. D. *J. Chem. Phys.* **1993**, *98*, 5648.

(39) Hamprecht, F.; Cohen, A. J.; Tozer, D. J.; Handy, N. C. *J. Chem. Phys.* **1998**, *109*, 71.

(40) Møller, C.; Plesset, M. S. *Phys. Rev. A* **1971**, *46*, 618.

(41) Kirshnan, R.; Pople, J. A. *Int. J. Quantum Chem.* **1978**, *14*, 91.

(42) Pople, J. A.; Head-Gordon, M.; Raghavachari, K. *J. Chem. Phys.* **1987**, *87*, 5968.

(43) Purvis, G. D., III; Bartlett, R. J. *J. Chem. Phys.* **1982**, *76*, 1910.

(44) Raghavachari, K.; Trucks, G. W.; Pople, J. A.; Head-Gordon, M. *Chem. Phys. Lett.* **1989**, *157*, 479.

(45) Dunning, T. H., Jr. *J. Chem. Phys*. **1989**, *90*, 1007.

(46) Dunning, T. H., Jr.; Harrison, R. J. *J. Chem. Phys*. **1992**, *96*, 6796.

(47) Frisch, M. J.; Trucks, G. W.; Schlegel, H. B.; Gill, P. M. W.; Johnson, B. G.; Robb, M. A.; Cheeseman, J. R.; Keith, T. A.; Petersson, G. A.; Montgomery, J. A.; Raghavachari, K.; Al-Laham, M. A.; Zakrzewski, V. G.; Ortiz, J. V.; Foresman, J. B.; Cioslowski, J.; Stefanov, B. B.; Nanayakkara, A.; Challacombe, M.; Peng, C. Y.; Ayala, P. A.; Chen, W.; Wong, M. W.; Andres, J. L.; Replogle, E. S.; Gomperts, R.; Martin, R. L.; Fox, D. J.; Binkley, J. S.; DeFrees, D. J.; Baker, J.; Stewart, J. J. P.; Head-Gordon, M.; Gonzalez, C.; Pople, J. A. *Gaussian 94*, revision B.3; Gaussian, Inc.: Pittsburgh, PA, 1995.

(48) Werner, H.-J.; Knowles, P. J.; Almlöf, J.; Amos, R. D.; Deegan, M. J. O.; Elbert, S. T.; Hampel, C.; Meyer, W.; Peterson, K.; Pitzer, R.; Stone, A. J.; Taylor, P. R.; Lindh, R.; Mura, M. E.; Thorsteinsson, T. *MOLPRO-97*; University of Birmingham: Birmingham, U.K., 1997.

(49) Amos, R. D.; Alberts, I. L.; Andrews, J. S.; Colwell, S. M.; Handy, N. C.; Jayatilaka, D.; Knowles, P. J.; Kobayashi, R.; Laidig, K. E.; Laming, G.; Lee, A. M.; Maslen, P. E.; Murray, C. W.; Rice, J. E.; Simandiras, E. D.; Stone, A. J.; Su, M.-D.; Tozer, D. J. *CADPAC: The Cambridge Analytic Derivative Package*, issue 6.5; University of Cambridge, U.K., 2000.

(50) Ahlrichs, R.; Bär, M.; Baron, H.-P.; Bauernschmitt, R.; Böcker, S.; Ehrig, M.; Eichkorn, K.; Elliot, S.; Haase, F.; Häser, M.; Horn, H.; Huber, C.; Huniar, U.; Kattannek, M.; Kölmel, C.; Kollwitz, M.; Ochsenfeld, C.; Öhm, H.; Schäfer, A.; Schneider, U.; Treutler, O.; von Arnim, M.; Weigend, F.; Weis, P.; Weiss, H. *TURBOMOLE*, version 4; Quantum Chemistry Group: University of Karlsruhe, Karlsruhe, Germany, 1997.

(51) Weigend, F.; Hässer, M. *Theor. Chim. Acta* **1997**, *97*, 331.